Polarized absorption spectroscopy of Λdoublet molecules: Transition moment vs electron density distribution

Laurence Bigio and Edward R. Grant

Citation: The Journal of Chemical Physics **87**, 5589 (1987); doi: 10.1063/1.453530
View online: http://dx.doi.org/10.1063/1.453530
View Table of Contents: http://scitation.aip.org/content/aip/journal/jcp/87/10?ver=pdfcov
Published by the AIP Publishing

Polarized absorption spectroscopy of Λ-doublet molecules: Transition moment vs electron density distribution

Laurence Bigio[a] and Edward R. Grant[b]
Department of Chemistry, Cornell University, Ithaca, New York 14853

(Received 23 June 1987; accepted 1 July 1987)

Polarized two-photon photodissociation of NO_2 in the region of 480 nm yields $NO(v'' = 0)$ with an anisotropic distribution of J. Measured polarization ratios are compared to quantum mechanical calculations for a range of expected ratios for the various isolated and mixed branches of the NO $\tilde{X}\,^2\Pi_{1/2} \rightarrow \tilde{A}\,^2\Sigma^+$ transition. Theoretical results show that main branches and their respective satellites (e.g., R_{11} and R_{21} branches) have the same transition moment directionally, though their intensities are in general different, implying that care is needed in interpreting polarization data from the mixed branches, such as $(Q_{21} + R_{11})$ or $(Q_{11} + P_{21})$, which measure the Π^+ and Π^- Λ doublet, respectively. Recognition of this fact is particularly important for properly separating the consideration of electron density distributions of Λ doublets from transition moment directionalities, as this has been a source of confusion in the literature. The measured results indicate that the principal two-photon photoexcitation pathway in NO_2 photolysis is $^2A_1 \rightarrow 1\,^2B_2 \rightarrow 2\,^2B_2$, with moderate A'' state mixing in the intermediate.

I. INTRODUCTION

Polarized absorption and emission spectroscopies enhance our understanding of photoexcitation–fragmentation processes by illuminating their vector properties. Product transition intensities, gathered as a function of pump–probe relative polarization, can be used to establish the presence of dissociation anisotropy and characterize the electronic transitions underlying parent photopreparation.[1–7] The specificity of polarization information has progressed with the resolution of state-to-state photolysis experiments. For some time, product alignments have been observed in spontaneous emission from excited photoproducts following photodissociation.[8–12] More recently, information has been added on ground state photoproduct polarizations in triatomic dissociations by laser-induced fluorescence.[13–15]

Access to higher-lying states and expanded opportunities for optical selection are offered by means of two-photon photolysis. Predicted alignments of photoprepared parents, following two-photon excitation have been summarized for bent→bent, bent→linear, and linear→linear transitions in triatomics.[11] However, comparatively few systems have been studied experimentally. Results of theoretical predictions have been used to assign the symmetry of the dissociating state in XeF_2 two-photon photolysis.[11,16] Similar arguments, based on classical limits for two-photon alignment, have been used for H_2O to establish strongly state-specific contributions from structured and continuum portions of the overlayed parent $\tilde{C}$ and $\tilde{B}$ states to the distribution of ground and excited state OH products.[12]

We have recently reported product NO ($X\,^2\Pi$) rotational and Λ-doublet state distributions following two-photon photodissociation of NO_2.[17] With a $^2\Pi$ product, this dissociation affords an opportunity to investigate the orientation of fragment unpaired electron density, in concert with the alignment of product angular momentum. These characteristics are, of course, related through their common dependence on angular momentum coupling hierarchies. This connection has lead to some confusion in the literature, concerning in particular the proper relationship between observed polarization ratios and the alignment of unpaired electron density (Λ-doublet selectivity) in spectroscopically probed products.

The most complete analysis presently available is that which has been constructed for the photodissociation of H_2O by Andresen and co-workers.[14b] While it draws from the data final conclusions about product orientation and electron density alignment that are correct for the specific transitions used, its approximate forms for spin–rotational wave functions of the Λ doublets and their transition moments, fail to accurately differentiate between mixed and isolated branches for $\Pi \rightarrow \Sigma$ transitions. As a result, the published formalism confuses the relationship between electron density distribution and transition moment directionality, and has thus limited general application. Correct and complete Λ-doublet wave function expressions have been included in more recent work by Andresen and Rothe,[18] as well as an insightful paper by Alexander and Dagdigian,[19] which includes a complete analysis of the cylindrical asymmetry of Λ-doublet electron density distributions.

In the present work we return to the question of transition moment directionality in $^2\Pi \rightarrow {}^2\Sigma$ transitions. Using complete and detailed wave functions for upper and lower electronic state spin–orbit–rotational angular momentum components, we derive general expressions for polarized intensities that apply to both isolated and mixed branches. We then use these expressions to address the question of alignment of the NO product plane of rotation following polarized two-photon photolysis of NO_2.

Photoproduct polarizations are determined in this work by one-plus-one ionization spectroscopy, in which the only relevant directionality is that determined by the relative po-

[a] Present address: General Electric Research and Center, P.O. Box 8, Bldg. K1-4C34, Schenectady, NY 12301.
[b] Address reprint requests to this author at: Department of Chemistry, Purdue University, West Lafayette, IN 47907.

larizations of the counterpropagating photolysis and probe beams. (We assume that the anisotropy associated with the transition induced by the second photon, which carries the NO to ionization, is negligible.[20–24]) We thus distinguish between this and previous work—in which the method of detection is fluorescence—by the fact that ionization in this case offers a detector with a nearly uniform 4π collection efficiency. Limiting predictions, compared with the experimental results, determine the nature of the photopreparation transition in the parent NO_2.

Our analysis begins with a complete discussion of the wave functions and matrix elements for $^2\Pi \rightarrow {}^2\Sigma^+$ transitions. The polarizations of the various branches, corresponding to either the Π^+ or Π^- Λ doublet, are shown to be strictly a function of ΔJ, rather than ΔN (where $\mathbf{J} = \mathbf{N} + \mathbf{S}$). Implications are discussed for polarization studies of mixed branches, such as $(Q_{11} + P_{21})$, and connection is made to the physical significance of the Λ doublets in terms of electron density distributions. Sections III and IV outline the details of the experimental arrangement pertinent to the polarization studies, and show the results for the polarization ratio, $R \equiv I_{\parallel}/I_{\perp}$. Finally, Sec. V discusses the meaning of the present results in terms of possible transitions in the parent NO_2.

II. THEORETICAL BACKGROUND

A. Ground state

Before discussing the polarization detection of nascent NO Λ-doublet states, it is worthwhile to briefly review the properties of the Λ-doublet wave functions. The ground state of NO is $^2\Pi$ with a single π electron forming the p lobes and defining the electronic symmetry. The wave functions for the $F_1 (J = N + 1/2)$ and $F_2 (J = N - 1/2)$ levels of this ground state can be written using a Hund's case (a) basis as[18,19,25]

$$|JMF_1 e/f\rangle = b_J |J,M,\Omega = 1/2,e/f\rangle + a_J |J,M,\Omega = 3/2,e/f\rangle, \quad (1a)$$

$$|JMF_2 e/f\rangle = -a_J |J,M,\Omega = 1/2,e/f\rangle + b_J |J,M,\Omega = 3/2,e/f\rangle, \quad (1b)$$

where

$$a_J = \left[\frac{X - (\lambda - 2)}{2X}\right]^{1/2}, \qquad b_J = \left[\frac{X + (\lambda - 2)}{2X}\right]^{1/2}, \quad (a_J^2 + b_J^2 = 1),$$

$$\lambda = A/B,$$

$$X = [4(J + 1/2)^2 + \lambda(\lambda - 4)]^{1/2},$$

and A is the spin–orbit splitting constant (123.26 cm^{-1} for NO) and B is the rotational constant (1.6725 cm^{-1} for $v'' = 0$).

The Λ-doublet wave functions are given by[19]

$$|JM\Omega,e/f\rangle = \frac{1}{\sqrt{2}} [|JM\Omega,\Lambda = 1,\Sigma = \pm 1/2\rangle + \epsilon |JM - \Omega,\Lambda = -1,\Sigma = \mp 1/2\rangle], \quad (2)$$

where the upper and lower signs refer to $\Omega = 3/2$ and $1/2$, respectively. The e Λ-doublet component corresponds to $\epsilon = +1$, and the f corresponds to $\epsilon = -1$, for both F_1 and F_2 levels. The electronic symmetry with respect to reflection through the plane of rotation (POR) is given by $+\epsilon$ for F_1, and $-\epsilon$ for F_2 levels, so that e levels have positive reflection symmetry in F_1 and negative in F_2, and vice versa for f levels.

B. Matrix elements and polarization ratio

The wave function for the $^2\Sigma^+$ state of NO is given in the case (a) basis as[26]

$$|JM\,{}^2\Sigma^+,\epsilon\rangle = \frac{1}{\sqrt{2}} [|JM\Omega = \Sigma = -\tfrac{1}{2}\rangle + \epsilon |JM\Omega = \Sigma = \tfrac{1}{2}\rangle], \quad (3)$$

where $\epsilon = +1$ corresponds to $F_1 (J = N + 1/2)$, and $\epsilon = -1$ corresponds to $F_2 (J = N - 1/2)$ spin–rotation levels. We will be interested in the matrix elements of the dipole operator P_q between the ground $^2\Pi$ and excited $^2\Sigma^+$ states. P_q is given by[27]

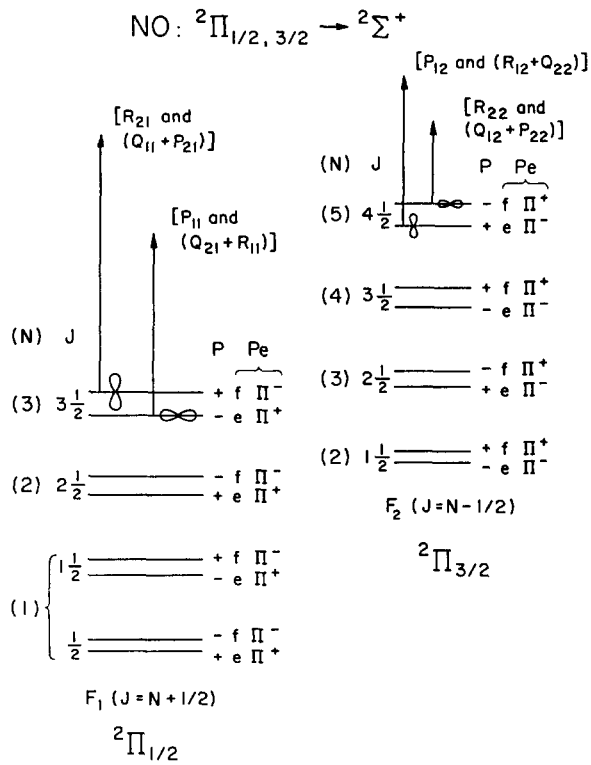

FIG. 1. Schematic level diagram for NO, showing J level, total parity P, and two conventional symbols used to define Λ-doublet components, e/f and $\Pi^+/^-$. The (+) and (−) superscripts specify positive and negative electronic symmetries Pe, with respect to reflection through any plane containing the internuclear axis. For high J, the plane of rotation is better defined, and Pe is designated with respect to this plane, so that in this limit states of Π^+ symmetry have the electron density of the single π electron concentrated in the plane of rotation, while Π^- states orient p lobes perpendicularly. This is shown schematically, even though, for low J, NO is primarily Hund's case (a) with little preferred electronic orientation. The rotational parity for case (a) is given by $P_B = (-1)^{J-\Omega}$, and its product with Pe gives the total parity P. The spin–orbit splitting is greater than that shown while the Λ splittings are much smaller (at low J approximately 0.01 cm^{-1} for the $^2\Pi_{1/2}$ state, and several MHz for the $^2\Pi_{3/2}$ state).

$$P_0 = P_z,$$
$$P_{\pm 1} = \mp\frac{1}{\sqrt{2}}(P_x \pm iP_y), \tag{4}$$

where P_x, P_y, and P_z are the Cartesian components of the dipole operator.

The allowed transitions are summarized in Fig. 1, which includes two conventional labels[28] for the ground state Λ doublets, as well as the total parities for those states. The parities of the $^2\Sigma^+$ states, connected by the branches shown, are always opposite the parities of the $^2\Pi$ states from whence the branches originate. A branch is designated as $\Delta J_{F'F''}$, where F' is either F_1 or F_2 for the $^2\Sigma^+$ state, and F'' is either F_1 or F_2 for the $^2\Pi$ state. For example, the branch R_{21} refers to a $\Delta J = +1$ transition from an F_1 level of the $^2\Pi$ state to an F_2 level of the $^2\Sigma^+$ state.

In determining the matrix elements of P_q, we will limit ourselves to the F_1 level of the ground state (F_2 levels may be calculated in an identical fashion) and will explicitly write the electronic angular momentum for the Σ^+ state and as $\Lambda = 0$. All excited state quantities will be primed.

Using Eqs. (1a), (2), and (3), we write

$$\begin{aligned}\langle {}^2\Sigma^+|P_q|{}^2\Pi F_1\rangle = \tfrac{1}{2}\big[\,&\langle J'M',\Lambda'=0,\Omega'=\Sigma'=-\tfrac{1}{2}| \pm \langle J'M',\Lambda'=0,\Omega'=\Sigma'=\tfrac{1}{2}|\,\big]\\ &\times P_q\big[\,b_J\big(|JM\Lambda=1,\Omega=\tfrac{1}{2},\Sigma=-\tfrac{1}{2}\rangle + \epsilon|JM\Lambda=-1,\Omega=-\tfrac{1}{2},\Sigma=\tfrac{1}{2}\rangle\big)\\ &+ a_J\big(|JM\Lambda=1,\Omega=\tfrac{3}{2},\Sigma=\tfrac{1}{2}\rangle + \epsilon|JM\Lambda=-1,\Omega=-\tfrac{3}{2},\Sigma=-\tfrac{1}{2}\rangle\big)\,\big].\end{aligned} \tag{5}$$

The $+$ sign of $\pm$ refers to F_1, and the $-$ sign to F_2 levels of the $^2\Sigma^+$ state.

To establish the polarization direction of the transition moment, we will need to compare

$|\langle {}^2\Sigma|P_0|{}^2\Pi\rangle|^2$ with $\frac{1}{2}(|\langle {}^2\Sigma|P_1|{}^2\Pi\rangle|^2 + |\langle {}^2\Sigma|P_{-1}|{}^2\Pi\rangle|^2)$.

It is easily shown for a given branch, that only one of the above matrix elements will be nonzero for a given choice of ϵ. It is for this reason that the various spectroscopic branches probe uniquely one or the other of the Λ-doublets components, as is shown in Fig. 1. Since no new information is conferred by retaining the $\epsilon|JM\Lambda=-1,\Omega,\Sigma\rangle$ pieces, we drop them with the understanding that the correct photoselection is that given in Fig. 1. (Strict inclusion merely adds a factor of 2 to the transition moment which is irrelevant in the determination of polarization ratios.) We can now write the matrix elements as

$$\begin{aligned}\langle {}^2\Sigma^+|P_q|{}^2\Pi F_1\rangle = &\tfrac{1}{2}\,b_J\,\langle J'M',\Lambda'=0,\Omega'=\Sigma'=-\tfrac{1}{2}|P_q|JM,\Lambda=1,\Omega=\tfrac{1}{2},\Sigma=-\tfrac{1}{2}\rangle\\ &\pm\tfrac{1}{2}\,a_J\,\langle J'M',\Lambda'=0,\Omega'=\Sigma'=\tfrac{1}{2}|P_q|JM,\Lambda=1,\Omega=\tfrac{3}{2},\Sigma=\tfrac{1}{2}\rangle,\end{aligned} \tag{6}$$

where the upper sign is for F_1 and the lower for F_2 levels of the $^2\Sigma^+$ state.

Now consider an external field which defines the z axis. In our case this reference field is most conveniently defined by the polarization axis of the photolysis beam. Polarized photolysis generates products with a nascent distribution of M states given by $W(J,M)$. For example, a $\cos^2\theta$ distribution would be given by $W(J,M) = M^2/[J(J+1)]$.

We now define the polarization ratio R for product NO as

$$R \equiv \frac{I_\parallel}{I_\perp} = \frac{\Sigma_M W(J,M)|\langle {}^2\Sigma^+|P_0|{}^2\Pi F_1\rangle|^2}{\Sigma_M[W(J,M)/2]\,[|\langle {}^2\Sigma^+|P_1|{}^2\Pi F_1\rangle|^2 + |\langle {}^2\Sigma^+|P_{-1}|{}^2\Pi F_1\rangle|^2]}. \tag{7}$$

$I_\parallel$ is the signal intensity when probe and photolysis polarizations are parallel; likewise $I_\perp$ is the relative signal intensity when the two beams have polarizations perpendicular to each other (with the photolysis polarization always defining the z axis).

The matrix elements of Eq. (6) are calculated using Eq. (27) of Ref. 27. The Clebsch–Gordan coefficients found in this equation are tabulated in Appendix I of Rose.[29] We assume that the reduced matrix element also found in this equation is independent of spin.[27] Listed here are the results for the parallel and perpendicular relative signal intensities for the Q, P, and R branches ($\Delta J = 0, -1, +1$, respectively). The polarization ratio may then be calculated by simply dividing $I_\parallel$ by $I_\perp$.

Q branches ($\Delta J = 0$):

$$I_\parallel = \sum_{M=-J}^{J} W(J,M)\left[b_J\frac{\sqrt{2}}{8}\left(\frac{M(2J+1)}{J(J+1)}\right) \pm a_J\frac{\sqrt{2}}{8}\left(\frac{M^2(2J-1)(2J+3)}{J^2(J+1)^2}\right)^{1/2}\right]^2, \tag{8a}$$

$$\begin{aligned}I_\perp = &\sum_{M=-J}^{J}\frac{W(J,M)}{2}\\ &\times\left\{\left[\frac{b_J}{8}\left(\frac{(J+M+1)(J-M)(2J+1)}{J^2(J+1)^2}\right)^{1/2} \pm \frac{a_J}{8}\left(\frac{(J+M+1)(J-M)(2J-1)(2J+3)}{J^2(J+1)^2}\right)^{1/2}\right]^2\right.\\ &\left.+\left[\frac{b_J}{8}\left(\frac{(J-M+1)(J+M)(2J+1)}{J^2(J+1)^2}\right)^{1/2} \pm \frac{a_J}{8}\left(\frac{(J-M+1)(J+M)(2J-1)(2J+3)}{J^2(J+1)^2}\right)^{1/2}\right]^2\right\},\end{aligned} \tag{8b}$$

where $+ = Q_{11}$ and $- = Q_{21}$.

P branches ($\Delta J = -1$):

$$I_{\parallel} = \sum_{M=-J}^{J} W(J,M) \left[b_J \frac{\sqrt{2}}{8} \left(\frac{(J-M)(J+M)}{J^2} \right)^{1/2} \pm a_J \frac{\sqrt{2}}{8} \left(\frac{(J-M)(J+M)(2J+3)}{J^2(2J-1)} \right)^{1/2} \right]^2, \tag{9a}$$

$$I_{\perp} = \sum_{M=-J}^{J} \frac{W(J,M)}{2} \left\{ \left[\frac{b_J}{8} \left(\frac{(J-M-1)(J-M)}{J^2} \right)^{1/2} \pm \frac{a_J}{8} \left(\frac{(J-M-1)(J-M)(2J+3)}{J^2(2J-1)} \right)^{1/2} \right]^2 + \left[\frac{b_J}{8} \left(\frac{(J+M)(J+M-1)}{J^2} \right)^{1/2} \pm \frac{a_J}{8} \left(\frac{(J+M)(J+M-1)(2J+3)}{J^2(2J-1)} \right)^{1/2} \right]^2 \right\}, \tag{9b}$$

where $+ = P_{11}$ and $- = P_{21}$.

R branches ($\Delta J = +1$):

$$I_{\parallel} = \sum_{M=-J}^{J} W(J,M) \left[b_J \frac{\sqrt{2}}{8} \left(\frac{(J-M+1)(J+M+1)}{(J+1)^2} \right)^{1/2} \pm a_J \frac{\sqrt{2}}{8} \left(\frac{(J-M+1)(J+M+1)(2J-1)}{(J+1)^2(2J+3)} \right)^{1/2} \right]^2, \tag{10a}$$

$$I_{\perp} = \sum_{M=-J}^{J} \frac{W(J,M)}{2} \left\{ \left[\frac{b_J}{8} \left(\frac{(J+M+1)(J+M+2)}{(J+1)^2} \right)^{1/2} \pm \frac{a_J}{8} \left(\frac{(J+M+1)(J+M+2)(2J-1)}{(J+1)^2(2J+3)} \right)^{1/2} \right]^2 + \left[\frac{b_J}{8} \left(\frac{(J-M+1)(J-M+2)}{(J+1)^2} \right)^{1/2} \pm \frac{a_J}{8} \left(\frac{(J-M+1)(J-M+2)(2J-1)}{(J+1)^2(2J+3)} \right)^{1/2} \right]^2 \right\}, \tag{10b}$$

where $+ = R_{11}$ and $- = R_{21}$.

C. Theoretical results

To illustrate the J dependence of the polarization ratio R, we choose a J directional distribution of $\cos^2\theta$. We thus imagine NO produced anisotropically with its J vectors primarily pointing in the $\pm z$ lab directions. We then set

$$W(J,M) = \frac{M^2}{J(J+1)}, \tag{11}$$

corresponding to the $\cos^2\theta$ distribution. The results for the Q, R, and P branches are shown in Fig. 2. It must be emphasized that the polarization ratio R is independent of whether one is probing a main branch or its satellite. Thus we see that the transition moment directionally is only dependent on ΔJ, *not* ΔN. For example Q_{21} and Q_{11} branches both have the same curve for R. This is *not* to be confused with the *relative* intensities of Q_{21} vs Q_{11} for a *set* polarization. In fact the main branches will always be more intense than their respective satellites. For example, $I_{\parallel}$ for Q_{11} will be greater than $I_{\parallel}$ for Q_{21}. To see this, we take for simplicity $M = J$. Then

$$\begin{aligned} \langle {}^2\Sigma^+ | P_0 | {}^2\Pi F_1 \rangle &= b_J \frac{\sqrt{2}}{8} \left[\frac{(2J+1)^2}{(J+1)^2} \right]^{1/2} \\ &\quad \pm a_J \frac{\sqrt{2}}{8} \left[\frac{(2J-1)(2J+3)}{(J+1)^2} \right]^{1/2} \\ &\simeq \frac{\sqrt{2}}{8} \left(\frac{(2J+1)}{(J+1)} \right) (b_J \pm a_J), \end{aligned} \tag{12}$$

where $+ = Q_{11}$ and $- = Q_{21}$. This approximation is good for moderate to high $J(\geqslant 10)$. Then, squaring:

$$\begin{aligned} |\langle {}^2\Sigma^+ | P_0 | {}^2\Pi F_1 \rangle|^2 &\simeq \frac{1}{32} \frac{(2J+1)^2}{(J+1)^2} (b_J^2 + a_J^2 \pm 2a_J b_J) \\ &= \frac{1}{32} \frac{(2J+1)^2}{(J+1)^2} [1 \pm (2c_J^2 - 1)], \end{aligned} \tag{13}$$

where $c_J^2 = 1/2 + a_J b_J$. We therefore obtain

$$|\langle {}^2\Sigma^+ | P_0 | {}^2\Pi F_1 \rangle|^2 \simeq \begin{cases} \frac{1}{16} \frac{(2J+1)^2}{(J+1)^2} c_J^2 & \text{for } Q_{11} \\ \frac{1}{16} \frac{(2J+1)^2}{(J+1)^2} d_J^2 & \text{for } Q_{21} \end{cases}, \tag{14}$$

where $d_J^2 = 1 - c_J^2$.

For pure Hund's case (b) $c_J^2 = 1$, while for pure case (a) $d_J^2 = c_J^2 = 1/2$. For all intermediate cases, therefore, c_J^2 will be greater than d_J^2. This result means that the intensities of main branches relative to respective sattelites will depend on λ through the c_J and d_J coefficients, and thus show proportions which are different for different $^2\Pi$ molecules. We will see later that c_J^2 and d_J^2 are directly related to the components of the electron density distribution.

Note, however, that the ratio R, as defined in Eq. (7), is insensitive to λ. That is, for a particular reference anisotro-

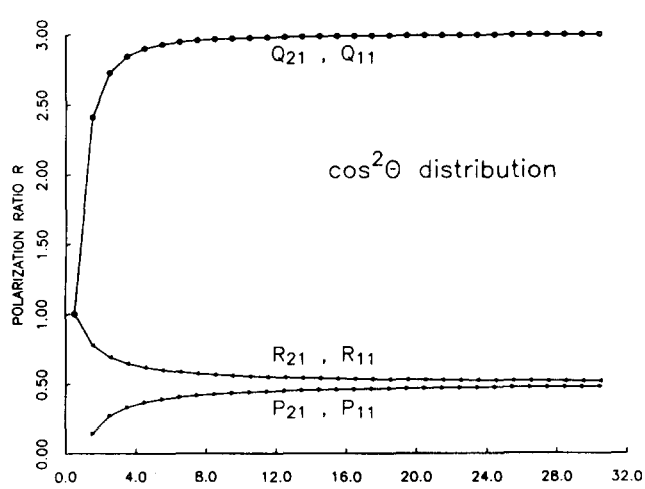

FIG. 2. Theoretical polarization ratio R for the six isolated F_1 level branches, computed for a $\cos^2\theta$ J distribution. Note that satellite and their respective main branch lines have the same values of R.

py, all $^2\Pi$ molecules undergoing a transition to $^2\Sigma^+$ will show the same R for a given *isolated* branch at a given J. At this point it is important to stress the word isolated, since, for each fine structure component, two pairs of branches each have very nearly degenerate transition energies. For the F_1 levels these are the $(Q_{21}+R_{11})$ and the $(Q_{11}+P_{21})$ bands. To properly consider the composite polarization ratio for the case when one of these *mixed* bands is being probed, one must add the contribution from each branch within the pair (recalling that their polarizations are opposite, as is seen in Fig. 2). *In this case*, the value of λ *is* very critical, and R is given, for example, by

$$R=\frac{I_{\parallel}(Q_{11})+I_{\parallel}(P_{21})}{I_{\perp}(Q_{11})+I_{\perp}(P_{21})}. \tag{15}$$

This is shown in Fig. 3, where R is plotted for the $(Q_{11}+P_{21})$ lines for $\lambda=3$, 10, and 74. Thus, different $^2\Pi$ molecules, such as NO or OH, *will* exhibit different polarization ratios as a function of J when such *mixed* branches are used for excitation. As mentioned above, however, for a given isolated branch, *all* $^2\Pi$ molecules with a given anisotropy will exhibit the *same* R as a function of J. This point has been the source of recent controversy. Andresen *et al.*[14(b)] assert that, for a given alignment, different $^2\Pi$ molecules with different λ will show different polarization ratios even for a given isolated branch, and that these differences follow the different electron density distributions for these molecules. They call this effect Λ mixing, referring to the mixed nature of the electron density distribution in and out of the plane of rotation. We claim that their approach confuses the relationship between transition dipole directionality and electron density. See Sec. II D for further discussion.

In Fig. 4 are shown the expected polarization ratios, assuming an initial $\cos^2\theta$ distribution of J, for the four branches typically seen in rotational spectra of NO (two of the branches are mixed). Note for low J, where Q_{21} carries the greater line strength factors,[27,30] that the $(Q_{21}+R_{11})$ branch shows R greater than unity. While for higher J, where the R_{11} carries the greater line strength factor, R falls to less than unity. Because Q_{21} is a satellite, its line strength

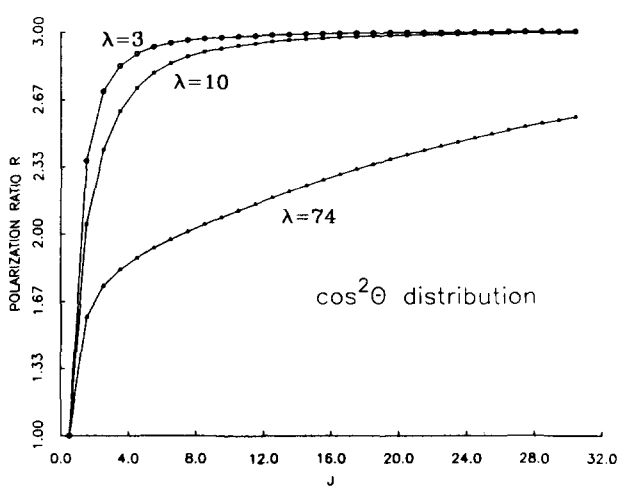

FIG. 3. Polarization ratio R for the $(Q_{11}+P_{21})$ mixed branch, given a $\cos^2\theta$ **J** distribution. Shown are curves of R for $\lambda=3$, 10, and 74, the last one of which is the λ appropriate to NO.

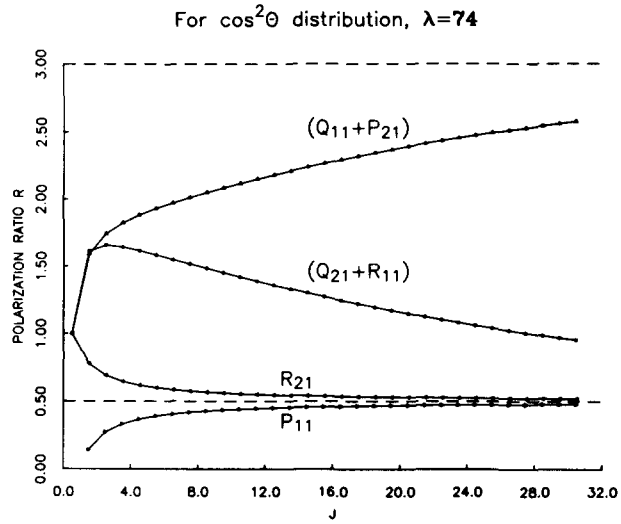

FIG. 4. Polarization ratio R from the four branches typically resolved in an NO($\lambda=74$) spectrum, given a $\cos^2\theta$ **J** distribution.

will eventually fall to zero, and the ratio R will approach 0.5 as for R_{21} and P_{11}.

Also shown on Fig. 4 are the dashed lines representing the classical high-J limiting value of the polarization ratio for Q and for P, R branches. These are evaluated in a straightforward manner by taking the dipole moment to be classical and aligned along J for Q branches and perpendicular to J, in the plane of rotation, for P, R branches. With reference to Fig. 5, the relative intensities for parallel versus perpendicular polarizations are given classically by the following expressions, where we explicitly show the $\cos^2\theta$ of **J** distribution.

For Q branches:

$$I_{\parallel}\propto\int_0^{2\pi}d\omega\int_0^{2\pi}d\phi\int_0^{\pi}(\cos^2\theta)\cos^2\theta\sin\theta\,d\theta$$
$$=\frac{8\pi^2}{5}, \tag{16a}$$

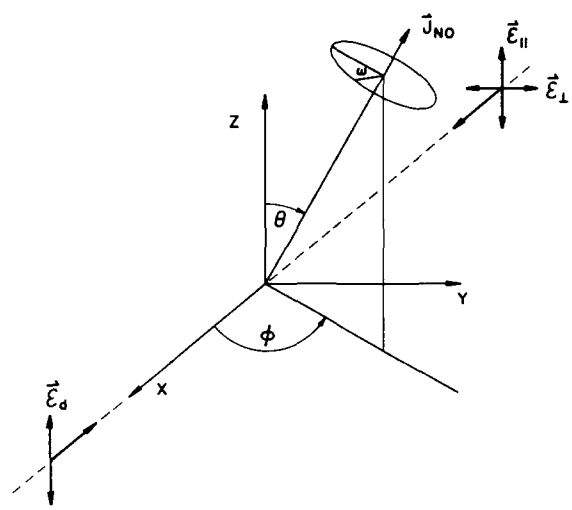

FIG. 5. Schematic showing the dissociation beam ϵ_d and the counterpropagating probe beam with polarization either parallel, $\epsilon_{\parallel}$, or perpendicular, $\epsilon_{\perp}$, to the polarization of ϵ_d. Also shown are the directions of $\mathbf{J}_{NO}$ in the lab-fixed frame.

$$I_\perp \propto \int_0^{2\pi} d\omega \int_0^{2\pi} \sin^2\phi d\phi \int_0^{\pi} (\cos^2\theta)\sin^2\theta \sin\theta\, d\theta$$
$$= \frac{8\pi^2}{15}, \quad (16b)$$
$$R_Q = \frac{I_\parallel}{I_\perp} = 3.$$

For P, R branches:

$$I_\parallel \propto \int_0^{2\pi} \cos^2\omega d\omega \int_0^{2\pi} d\phi \int_0^{\pi} (\cos^2\theta)\sin^2\theta \sin\theta\, d\theta$$
$$= \frac{8\pi^2}{15}, \quad (17a)$$
$$I_\perp \propto \int_0^{2\pi}\int_0^{2\pi}\int_0^{\pi} (\cos^2\theta)[\sin\phi\cos\theta\cos\omega + \sin\omega\cos\phi]^2 \sin\theta\, d\theta\, d\phi\, d\omega = \frac{16\pi^2}{15}, \quad (17b)$$
$$R_{P,R} = \frac{I_\parallel}{I_\perp} = 1/2.$$

D. Electron density

We now turn to the physical significance of the Λ doublets in terms of their electron density distribution. As originally discussed by Gwinn *et al.*,[31] these distributions are characterized by the expectation value of the operator $(x^2 - y^2) \propto (\cos^2\phi - \sin^2\phi)$, where ϕ is the azimuthal angle made by the π electron density about the internuclear z axis. We adopt the convention $|M| = J \gg 1$, which makes yz (body-fixed) the plane of rotation (see Ref. 19). The angle ϕ is measured from the x axis. The expectation value is defined as Δ and is given by[18,19] (for $M = J$)

$$\Delta = \langle {}^2\Pi|\cos^2\phi - \sin^2\phi|{}^2\Pi\rangle = \mp(\epsilon) a_J b_J S, \quad (18)$$

where $S = [(J - 1/2)/(J + 3/2)]^{1/2}$ and where the $-$ sign refers to F_1 and $+$ to F_2 levels. (For a π^3 occupancy molecule the signs would be reversed.) For high J, $a_J \approx b_J \approx 1/\sqrt{2}$ and $S \simeq 1$; then $\Delta \sim +0.5$ for $\epsilon = -$ (that is, for Π^- Λ doublets), and the electron density is primarily *out* of the POR, pointing along J. For $\epsilon = +$ (Π^+ Λ doublets), $\Delta \sim -0.5$ and the electron density is primarily *in* the POR, perpendicular to J. This is shown schematically by the symbols attached to the Λ doublets in Fig. 1.

Another way to see the ϕ dependence of the Λ-doublet wave functions is to rewrite Eqs. (1) and (2) making use of the fact that the eigenfunction for $|\Lambda = \pm 1\rangle$ has the form $e^{\pm i\phi}$, and this, in turn, can be written as $\cos\phi \pm i\sin\phi$. As discussed in Ref. 18, the square of the resulting wave function can than be integrated over all coordinates except for ϕ to yield the electron density $\rho(\phi)$ which has the form

$$\rho(\phi) \sim c_J^2 \sin^2\phi + d_J^2 \cos^2\phi \quad (\Pi^+),$$
$$\rho(\phi) \sim c_J^2 \cos^2\phi + d_J^2 \sin^2\phi \quad (\Pi^-), \quad (19)$$

where

$$c_J^2 = 0.5 + |\Delta|,$$
$$d_J^2 = 0.5 - |\Delta|.$$

Note that c_J^2 and d_J^2 are the same as for Eq. (13) except for the factor of S in Eq. (18), which quickly approaches 1 for moderately high J.

Summarizing these results, we have that for low J, $\Delta \sim 0$ and $c_J^2 \sim d_J^2 \sim 1/2$, so that the electron density is essentially cylindrically symmetric. This corresponds to the case (a) limit. At higher J, as the molecule takes on more case (b) character, the electronic density distribution becomes preferentially oriented in the POR for Π^+ Λ doublets, and perpendicular to the POR for Π^- Λ doublets. The extent to which a given Λ doublet has electron density principally directed either in or out of the plane is given by the mixing coefficients c_J^2 and d_J^2 in a manner that depends on which Λ doublet is under consideration, as is clear in Eq. (19).

Finally, as mentioned above, the extent of Λ mixing bears no relation to the directionality of individual transition moments. For example, despite the fact that R_{21} and Q_{11} both gauge the Π^- Λ doublet, their polarization directions will be opposite. The only case where Λ mixing *is* important is when a *mixed* branch, such as $(Q_{11} + P_{21})$, is measured due to the typical inability to resolve the individual branches of such a pair. Then, the fact that these two branches have opposite polarizations, will dramatically effect any measurement made for the polarization ratio R. For example, in the specific case of $(Q_{11} + P_{21})$, the relative weight of the Q_{11} contribution will be $4c_J^2$, and that of P_{21} will be d_J^2 (at moderate to high J). Therefore, measurements of R should always be done on isolated branches whenever possible.

As already noted, this last point has been the source of some confusion in the literature. For example, Eq. (3) of Ref. 18 and Eq. (12) of Ref. 14(b) give a prescription for determining the electron density. Those equations, however, are used improperly as wave functions in Eq. (22) of Ref. 14(b) and the "Polarization Effects" section of Ref. 18. Such functions are not appropriate as representations of the lower state for deriving transition moment directionality, because they ignore crucial information imparted by the quantum numbers J, M, Λ, Ω, and Σ.[32] Most seriously, the formalism established by Eq. (22) of Ref. 14(b) fails to discriminate between *isolated* main and satellite branches and *mixed* branches [e.g., $(Q_{11} + P_{21})$]. Conclusions expressed there, relating degree of alignment to observed polarization ratio as a function of J, would be qualitatively correct only insofar as the mixed Q branches, $(Q_{11} + P_{21})$ and $(R_{12} + Q_{22})$, are concerned. In this case, observed polarization behavior will follow J in a manner that varies from molecule to molecule depending on λ as illustrated by Fig. 3. Missing in the treatment of Ref. 14(b) is the fact that transitions of both $\Delta J = 0$ and $\Delta J = \pm 1$ exist for each Λ doublet. These yield opposite transition moment directionalities, even though the electron density being probed within each set of transitions that originate from the same Λ doublet is obviously the same.

III. EXPERIMENTAL SECTION

The experimental arrangement used for the polarization study of the nascent NO states is identical to that described in Ref. 17. Briefly a free jet of NO_2 (1:1:20 seeded; NO_2:O_2:Ar) is crossed by the focused counterpropagating outputs of the photolysis (pump) and probe beams. The

two-photon dissociation of NO_2 just above the $O(^1D)$ threshold generates product states of NO that are vibrationally cold ($v'' = 0$) for the $O(^1D)$ channel. The rotational and Λ-doublet distributions of the nascent NO are studied by conventional $1 + 1$ ionization spectroscopy employing the $X\,^2\Pi \rightarrow A\,^2\Sigma^+$ transition.

Of particular relevance to the polarization measurements is the Pockels cell (Lasermetrics DKDP) used to rotate the relative polarization directions between the pump and probe beams. In this case it is placed in the pump beam path just before the molecular beam chamber. No loss of total intensity is measured as a function of applied voltage to the cell. For 487 nm light with vertical input polarization and an applied voltage of 3000 V, we find more than 95% of the output horizontally polarized. No distortion of the original polarization occurs for zero applied voltage. Alignment of the cell is critical and was expedited using sensitive x, y, z tilters and translation stages.

The overlapping arrangement of the foci of the two beams is also critical and is accomplished using x, y positioners for the two focusing lenses. Possible distortion of the exact overlap due to the Pockels cell was tested by checking $I_\parallel$ vs $I_\perp$ for $J = 1/2$. For $J = 1/2$, no polarization difference would be expected, and so any change in the signal would indicate a movement of the pump beam focus, and therefore a fault in the Pockels cell alignment. No change was found as the voltage was varied smoothly from 0 to 3000 V, indicating no misalignment. (In fact polarization differences only start to appear in the R_{21} branch for $J > 11.5$; see Sec. IV.) These results, given the relative ease of alignment of the Pockels cell (using the x, y, z tilters) show its distinct usefulness for polarization measurements for cases, such as focused photolysis or ionization detection of products, where alignment of pump and probe beams is critical.

IV. RESULTS

Two bands have been chosen to obtain the polarization ratio, R_{21} and $(Q_{21} + R_{11})$, because their high-J lines occur in the least conjested part of the NO spectrum. Several two-photon photolysis wavelengths have been examined (484.79, 479.05, and 471.22 nm) and found to give essentially the same results. The particular wavelengths were chosen to maximize the available signal by resting on peaks in the two-photon photolysis spectrum of the NO_2. Such a spectrum is shown for the 471 nm region in Fig. 6.

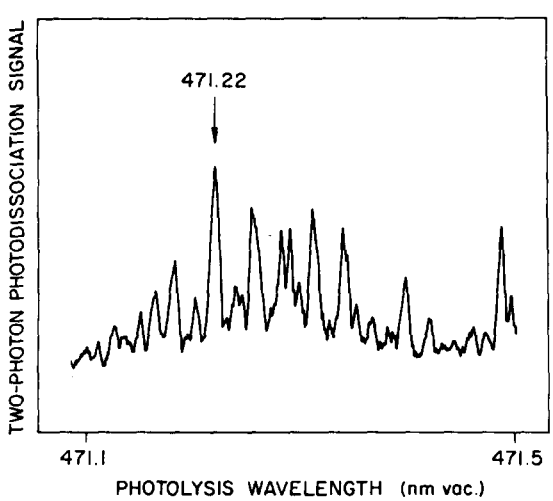

FIG. 6. Two-photon photodissociation spectrum of NO_2. Structure is indicative of the NO_2 intermediate state structure. Arrow indicates the peak at which the photolysis wavelength is set for measurements of the polarization ratio for $J > 20.5$.

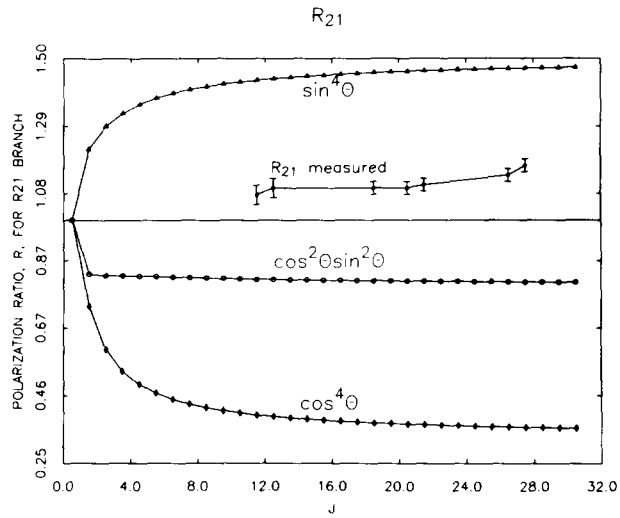

FIG. 7. Comparison of measured polarization ratio R for the R_{21} branch with three possible two-photon generated J distributions for that branch.

The measured ratios, $R = I_{11}/I_\perp$, are given in Figs. 7 and 8 for the R_{21} and $(Q_{21} + R_{11})$ branches, respectively. Also shown are the theoretical results calculated in the manner discussed in Sec. II for a $\sin^4\theta$, $\cos^4\theta$, and $\cos^2\theta \sin^2\theta$ distribution of J. These are meant to model the three possible limiting distributions for a two-photon transition, assuming an ideal and instantaneous planar dissociation, and will be discussed further in the next section.

For all the cases studied, it is found that all energetically allowed NO rotational states are populated, with population dropping sharply for states of energy higher than the excess two-photon photolysis energy for the production of $O(^1D)$, indicating a relatively cold initial state distribution, and dissociation dynamics for $NO(v'' = 0)$ determined exclusively by the energetics of the $O('D)$ channel.

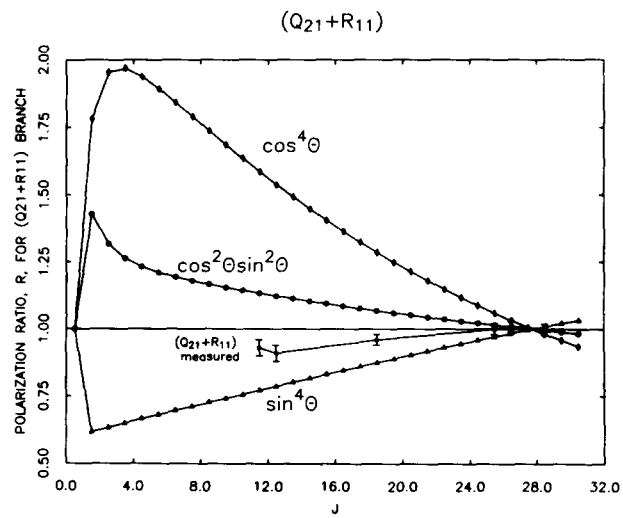

FIG. 8. Comparison of measured polarization ratio R for the $(Q_{21} + R_{11})$ mixed branch with three possible two-photon generated J distributions for that branch.

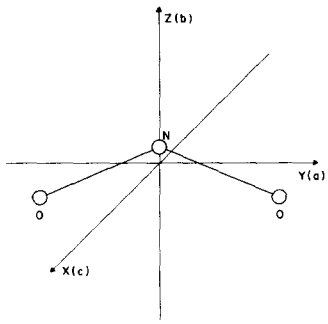

FIG. 9. Near-prolate axes directions for NO_2.

V. DISCUSSION

Spectroscopic language distinguishes parallel from perpendicular transitions for bent triatomic molecules according to their effect on the K quantum number. Referring to Fig. 9 for NO_2 (a near-prolate top), transitions with moments that lie along the top axis a (y) are parallel, with $\Delta K = 0$, while those with moments that lie along b or c (z or x) are perpendicular, with $\Delta K = \pm 1$. In dissociation dynamics, however, the reference is generally taken to be the plane of the triatomic prior to dissociation. For fast dissociations of low angular momentum triatomics, the rotation plane of the diatom is the same as the original triatomic plane, designated as Δ.[4] Thus, transitions exciting in plane moments along a or b ($\|\Delta$) produce a $\sin^2\theta$ product J distribution with respect to photolysis polarization. Transitions exciting the perpendicular moment along c ($\perp\Delta$) produce a $\cos^2\theta$ distribution of J vectors.

The six possible two-photon transitions for NO_2 are listed below together with the J distribution predicted for each[33]:

$$^2A_1 \underset{\|\Delta}{\rightarrow} {}^2B_2 \underset{\|\Delta}{\rightarrow} {}^2B_2 \quad \sin^4\theta, \tag{20}$$

$$^2A_1 \underset{\|\Delta}{\rightarrow} {}^2B_2 \underset{\perp\Delta}{\rightarrow} {}^2A_2 \quad \cos^2\theta \sin^2\theta, \tag{21}$$

$$^2A_1 \underset{\|\Delta}{\rightarrow} {}^2B_2 \underset{\|\Delta}{\rightarrow} {}^2A_1 \quad \sin^4\theta, \tag{22}$$

$$^2A_1 \underset{\perp\Delta}{\rightarrow} {}^2B_1 \underset{\|\Delta}{\rightarrow} {}^2B_1 \quad \cos^2\theta \sin^2\theta, \tag{23}$$

$$^2A_1 \underset{\perp\Delta}{\rightarrow} {}^2B_1 \underset{\|\Delta}{\rightarrow} {}^2A_2 \quad \cos^2\theta \sin^2\theta, \tag{24}$$

$$^2A_1 \underset{\perp\Delta}{\rightarrow} {}^2B_1 \underset{\perp\Delta}{\rightarrow} {}^2A_1 \quad \cos^4\theta. \tag{25}$$

The intermediate state region of NO_2 accessed by the first photon is composed of vibronic states whose characters contain mixtures of the four low-lying electronic states. Oscillator strength for transitions from the ground $^2A_1$ state is carried by the $1\,^2B_2$ and $1\,^2B_1$ electronic states, with $1\,^2B_2$ found to dominate most regions in the visible spectrum that have been studied.[34] The only known state in the region accessed by the second photon is the $2\,^2B_2$ state, whose origin at 40 126 cm^{-1} lies 872 cm^{-1} below the $O(^1D)$ threshold which is 40 998 cm^{-1}. This state is predissociated at the origin with a lifetime of 42 ps.[35] This lifetime decreases rapidly with increased energy. Rotational structure becomes completely diffuse by 40 850 cm^{-1},[36] and it is inferred that the lifetime is subpicosecond by the energy region of the $O(^1D)$ threshold. If the final electronic state in the present photolysis is indeed $2\,^2B_2$, and the intermediate is $1\,^2B_2$, then the principal excitation path will be Eq. (20) above, with a resulting $\sin^4\theta J$ distribution.

The results of Figs. 7 and 8 show that the measured polarization ratios more closely match a $\sin^4\theta$ distribution than a $\cos^2\theta \sin^2\theta$ or $\cos^4\theta$ distribution. That is, the J vectors of the nascent NO are produced in an aligned fashion predominantly perpendicular to the polarization direction of the photolysis beam. This conclusion is confirmed by the consistency of the results for the two separate branches, R_{21} and $(Q_{21} + R_{11})$. What might be thought of as surprising that the $(Q_{21} + R_{11})$ branch shows less polarization difference for higher J than the R_{21} does, is actually seen to be due to the opposing polarization directions of the Q_{21} and R_{11} partners. For low J, where Q_{21} carries most of the line strength, the polarization ratio displays what would be expected for a Q branch. At higher J, where R_{11} has the larger line strength, the ratio crosses $R = 1$ and starts to approach the limit for an R branch.

The fact that there is any deviation from an $R = 1$ measured ratio allows one to put certain limits on the nature of the two-photon transition, as well as the time scale for dissociation. Since the polarization measurements which were taken at several different photolysis wavelengths give consistent results, the above mentioned similarity to the $\sin^4\theta$ distribution shows the most likely set of electronic transitions to be $^2A_1 \rightarrow {}^2B_2 \rightarrow {}^2B_2$. This result is supported by the recent double resonance work of Tsukiyama *et al.* who excite with λ_1 at 471.4 nm and λ_2 at 518 nm to reach the $2\,^2B_2$ origin.[37] Their results, consistent with those of Smalley *et al.*[38] indicate the intermediate to be $^2B_2$. Any mixing of B_1 character, however, in the intermediate state, or of B_1, A_2, or A_1 character in the final state, will result in a depolarization from the expected $\sin^4\theta$ distribution. Yet even for a well defined set of transitions, results may be extensively depolarized if the dissociation lifetime is greater than a typical rotational period. The fastest rotations induced (largest rotation constant) are those in which K is excited, implying a rotation about the axis (a), with a period of $h/\Delta\nu \sim 2$ ps. Thus, an upper limit to the lifetime of the dissociative state is on the order of a ps. Since the diffuse spectra indicate that, in fact, the lifetime is much shorter than this, one is left to conclude that the reason for the observed depolarization is not caused by a long dissociative lifetime, but rather to a moderate amount of state mixing in either the intermediate or final states of the NO_2.[39] Earlier work[40] has speculated on the existence of a linear $^2\Sigma_g^+$ state in the energy region 5840 cm^{-1} above the $O(^1D)$ threshold in order to explain rotationally cold NO product state distributions. However, for the energy region of 0–1400 cm^{-1} in which the present work has been conducted, it is found that all energetically allowed rotational states are populated. Since only relatively low angular momentum states of the jet-cooled NO_2 are excited, the highly rotationally excited products must arise solely from the dynamics of the dissociation itself. The data, thus, do not evidence crossing to a linear, totally symmetric state for energies less than 1400 cm^{-1} above the $O(^1D)$ threshold. Similarly, Tsukiyama *et al.*[37] and Hallin and Merer[35] show no evidence for state mix-

ing near the origin of the $2\,^2B_2$ level. We therefore conclude that the final $2\,^2B_2$ state is relatively unperturbed, and that depolarization must result primarily from state mixing at the intermediate level. This mixing may be understood more appropriately in C_s symmetry. The A_1/B_2 conical intersection forms A' levels, whereas the A_1/B_1 Renner–Teller pair form A'' levels. Any A'' mixing in the intermediate, originating from the B_1 state, would result in a depolarization of both the first and second photon steps, since $A' \leftrightarrow A''$ are perpendicular transitions. Thus, the results imply a primarily B_2 intermediate, but with nonnegligible A'' character most probably mixed in by Coriolis interactions.

VI. SUMMARY

We have developed the quantum mechanical calculations necessary for correctly analyzing the polarization dependencies expected for the various isolated and mixed branches of the NO $X\,^2\Pi_{1/2} \rightarrow A\,^2\Sigma^+$ transition. The results are general for all $^2\Pi$ molecules undergoing a transition to a $^2\Sigma^+$ state, and may be extended to other transitions with slight modifications. We find that main branches, such as Q_{11}, have the same transition moment directionality as their respective satellite branches, such as Q_{21}, although their intensities are in general different. This means that careful interpretation is needed in analyzing polarization data from mixed bands such as the $(Q_{21} + R_{11})$ or $(Q_{11} + P_{21})$, which measure the Π^+ and Π^- Λ doublet, respectively. We have shown how to properly analyze such mixed bands, and have applied these results to the two-photon photodissociation of NO_2 followed by $1 + 1$ ionization detection of the nascent NO. Comparison of experimental product alignments with theory indicates that the principal two-photon photodissociation pathway for excitation just above the $O(^1D)$ threshold in NO_2 is $^2A_1 \rightarrow 1\,^2B_2(A') \rightarrow 2\,^2B_2$ with moderate A'' character mixing in the intermediate.

ACKNOWLEDGMENTS

We are grateful to M. H. Alexander, P. Andresen, and P. J. Dagdigian for helpful discussions. This work was supported by the U. S. Army Research Office.

[1]R. J. Van Brunt and R. N. Zare, J. Chem. Phys. **48**, 4304 (1968).
[2]M. T. Macpherson, J. P. Simons, and R. N. Zare, Mol. Phys. **38**, 2049 (1979).
[3]G. W. Loge and R. N. Zare, Mol. Phys. **43**, 1419 (1981).
[4]G. W. Loge, Mol. Phys. **47**, 225 (1982).
[5]C. H. Green and R. N. Zare, J. Chem. Phys. **78**, 6741 (1983).
[6]T. Nagata, T. Kondow, K. Kuchitsu, G. W. Loge, and R. N. Zare, Mol. Phys. **50**, 49 (1983).
[7]R. Altkorn and R. N. Zare, Annu. Rev. Phys. Chem. **35**, 265 (1984).
[8]G. A. Chamberlain and J. P. Simons, Chem. Phys. Lett. **32**, 355 (1975); J. Chem. Soc. Faraday Trans. 2 **71**, 2043 (1975); M. T. Macpherson and J. P. Simons, Chem. Phys. Lett. **51**, 261 (1977); J. P. Simons and A. J. Smith, *ibid.* **97**, 1 (1983); J. P. Simons, A. J. Smith, and R. N. Dixon, J. Chem. Soc. Faraday Trans. 2 **80**, 1489 (1984).
[9]M. T. Macpherson and J. P. Simons, J. Chem. Soc. Faraday Trans. 2 **74**, 1965 (1978); **75**, 1572 (1979); M. N. R. Ashfold, A. S. Georgiou, A. M. Quinton, and J. P. Simons, *ibid.* **77**, 259 (1981).
[10]E. D. Poliakoff, S. H. Southworth, D. A. Shirley, K. H. Jackson, and R. N. Zare, Chem. Phys. Lett. **65**, 407 (1979).
[11]G. W. Loge and J. R. Wiesenfeld, J. Chem. Phys. **75**, 2795 (1981).
[12]A. Hodgson, J. P. Simons, M. N. R. Ashfold, J. M. Bayley, and R. N. Dixon, Mol. Phys. **54**, 351 (1985).
[13]R. Vasudev, R. N. Zare, and R. N. Dixon, Chem. Phys. Lett. **96**, 399 (1983); R. Vasudev, R. N. Zare, and R. N. Dixon, J. Chem. Phys. **80**, 4863 (1984).
[14](a) P. Andresen and E. W. Rothe, J. Chem. Phys. **78**, 989 (1983); (b) P. Andresen, G. S. Ondrey, B. Titze, and E. Rothe, *ibid.* **80**, 2548 (1984).
[15]G. E. Hall, N. Sivakumar, and P. L. Houston, J. Chem. Phys. **84**, 2120 (1986).
[16]G. W. Loge and J. R Wiesenfeld, Chem. Phys. Lett. **78**, 32 (1981).
[17]L. Bigio and E. R. Grant, J. Chem. Phys. **87**, 360 (1987); J. Phys. Chem. **89**, 5855 (1985).
[18]P. Andresen and E. W. Rothe, J. Chem. Phys. **82**, 3634 (1985).
[19]M. H. Alexander and P. J. Dagdigian, J. Chem. Phys. **80**, 4325 (1984).
[20]The M_J dependence of the total cross section for one-photon ionization of NO ($A\,^2\Sigma^+$, $J = 14.5$) has been shown to range over less than 8% (see Refs. 21 and 22). Other work (Ref. 22) shows similar small M_J dependence for ionization of excited H_2. Given that $X \rightarrow A$ transitions prepare a distribution of M_J excited states, such a sensitivity to alignment upon ionization would alter apparent populations as probed by Q vs P or R branch transitions by an amount small compared to the present experimental error of 5%–10%. Though one report (Ref. 23) shows R (and presumably P) branches enhanced over Q branches for isotropic NO, the data displayed by Zacharias *et al.* (Ref. 24), as well as our own cursory examination of cold NO from a jet, show no such preferences (see Ref. 17). These discrepancies indicate, as pointed out in Ref. 21, that care is needed to avoid saturation which could produce the enhancement effects seen in Ref. 23.
[21]D. C. Jacobs and R. N. Zare, J. Chem. Phys. **85**, 5457 (1986); D. C. Jacobs, R. J. Madix, and R. N. Zare, *ibid.* **85**, 5469 (1986).
[22]S. N. Dixit and H. Rudolf (private communication).
[23]J. P. Booth, S. L. Bragg, and G. Hancock, Chem. Phys. Lett. **113**, 509 (1985).
[24]H. Zacharias, M. M. T. Loy, P. A. Roland, and A. S. Sudbo, J. Chem. Phys. **81**, 3148 (1984).
[25]M. H. Alexander and G. C. Corey, J. Chem. Phys. **84**, 100 (1986).
[26]M. H. Alexander, S. L. Davis, and P. J. Dagdigian, J. Chem. Phys. **83**, 556 (1985).
[27]R. J. M. Bennett, Mon. Not. R. Astron. Soc. **147**, 35 (1970).
[28]J. M. Brown, J. T. Hougen, K-P. Huber, J. W. C. Johns, I. Kopp, H. Lefebvre-Brion, A. J. Merer, D. A. Ramsay, J. Rostas, and R. N. Zare, J. Mol. Spectrosc. **55**, 500 (1975).
[29]M. E. Rose, *Elementary Theory of Angular Momentum* (Wiley, London, 1957).
[30]L. T. Earls, Phys. Rev. **48**, 423 (1935).
[31]W. D. Gwinn, B. E. Turner, W. M. Goss, and G. L. Blackman, Astron. J. **179**, 789 (1973).
[32]The problem with the analysis of Ref. 18 can be traced in its Appendix. Wave functions are properly given as Eqs. (A1) and (A5). The electron density map can be derived from Eq. (A8), which is the modulus square of Eq. (A5). However, its *square root*, offered as Eq. (3) in the text is *not* a proper wave function.
[33]These may also be read as overall vibronic transitions.
[34]For a comprehensive summary of NO_2 spectroscopy see: (a) D. K. Hsu, D. L. Monts, and R. N. Zare, *Spectral Atlas of Nitrogen Dioxide 5530 to 6480 Å* (Academic, New York, 1978); (b) K. Uehara and H. Sasada, *High Resolution Spectral Atlas of Nitrogen Dioxide 559–597 nm* (Springer, Berlin, 1985).
[35]K.-E. J. Hallin and A. J. Merer, Can. J. Phys. **54**, 1157 (1976).
[36]W. M. Uselman and E. K. C. Lee, Chem. Phys. Lett. **30**, 212 (1975). See also G. Herzberg, *Electronic Spectra of Polyatomic Molecules* (Van Nostrand–Reinhold, New York, 1966), pp. 482–483.
[37]K. Tsukiyama, K. Shibuya, K. Obi, and I. Tanaka, J. Chem. Phys. **82**, 1147 (1985).
[38]R. E. Smalley, L. Wharton, and D. H. Levy, J. Chem. Phys. **63**, 4977 (1975).
[39]Distributions of NO oriented by photoproduction are slowly depolarized for low J by nuclear hyperfine coupling. This effect is neglected here because: (1) NO products are probed within 15 ns of production, a time judged too short for depolarization given the magnitude of nuclear hyperfine splitting in NO, and (2) polarization in our experiments is only observed (indeed only meaningful) for high J, at which point nuclear spin depolarization effects are even smaller. See: F. A. Blum, K. W. Nill, A. R. Calawa, and T. C. Harman, Chem. Phys. Lett. **15**, 144 (1972); J. A. Guest, M. A. O'Halloran, and R. N. Zare, *ibid.* **103**, 261 (1984), and Ref. 21.
[40]R. J. S. Morrison and E. R. Grant, J. Chem. Phys. **77**, 5994 (1982).